JOURNAL OF GEOPHYSICAL RESEARCH, VOL. 114, D06116, doi:10.1029/2008JD011208, 2009

Annual accumulation for Greenland updated using ice core data developed during 2000–2006 and analysis of daily coastal meteorological data

Roger C. Bales,[1,2] Qinghua Guo,[1,2] Dayong Shen,[1] Joseph R. McConnell,[3] Guoming Du,[1] John F. Burkhart,[1,4] Vandy B. Spikes,[5] Edward Hanna,[6] and John Cappelen[7]

Received 26 September 2008; revised 12 December 2008; accepted 2 January 2009; published 27 March 2009.

[1] An updated accumulation map for Greenland is presented on the basis of 39 new ice core estimates of accumulation, 256 ice sheet estimates from ice cores and snow pits used in previous maps, and reanalysis of time series data from 20 coastal weather stations. The period 1950–2000 is better represented by the data than are earlier periods. Ice-sheet-wide accumulation was estimated based on kriging. The average accumulation (95% confidence interval, or ±2 times standard error) over the Greenland ice sheet is 30.0 ± 2.4 g cm^{-2} a^{-1}, with the average accumulation above 2000-m elevation being essentially the same, 29.9 ± 2.2 g cm^{-2} a^{-1}. At higher elevations the new accumulation map maintains the main features shown in previous maps. However, there are five coastal areas with obvious differences: southwest, northwest, and eastern regions, where the accumulation values are 20–50% lower than previously estimated, and southeast and northeast regions, where the accumulation values are 20–50% higher than previously estimated. These differences are almost entirely due to new coastal data. The much lower accumulation in the southwest and the much higher accumulation in the southeast indicated by the current map mean that long-term mass balance in both catchments is closer to steady state than previously estimated. However, uncertainty in these areas remains high owing to strong gradients in precipitation from the coast inland. A significant and sustained precipitation measurement program will be needed to resolve this uncertainty.

Citation: Bales, R. C., Q. Guo, D. Shen, J. R. McConnell, G. Du, J. F. Burkhart, V. B. Spikes, E. Hanna, and J. Cappelen (2009), Annual accumulation for Greenland updated using ice core data developed during 2000–2006 and analysis of daily coastal meteorological data, *J. Geophys. Res.*, *114*, D06116, doi:10.1029/2008JD011208.

1. Introduction

[2] Recent evidence suggests that Greenland's ice may be moving toward the sea much faster than previously estimated [*Zwally et al.*, 2002; *Rignot and Kanagaratnam*, 2006] and that the Greenland Ice Sheet is responding to a global-warming signal and warmer surrounding ocean water since the early 1990s [*Hanna et al.*, 2008, 2009]. Estimates of ice sheet mass balance depend in part on estimates of accumulation, or precipitation minus evaporation ($P-E$), as well as rates of mass wastage to the sea and ice sheet elevation changes. Errors and uncertainty in annual accumulation across the ice sheet propagate through to flux-based estimates [*Thomas et al.*, 2001; *Rignot et al.*, 2004] of overall ice sheet mass balance and impact interpretation of repeat altimetry-based mass balance estimates [*McConnell et al.*, 2000a; *Davis et al.*, 2005].

[3] Early estimates of ice sheet accumulation were based on records from snow pits, near-surface measurements and a limited number of coastal weather stations [*Benson*, 1962] and gave values in the range of 34 g cm^{-2} a^{-1} for the ice sheet. *Ohmura and Reeh* [1991] blended additional ice core records and coastal weather station data in order to estimate accumulation across the ice sheet, giving an average of 31 g cm^{-2} a^{-1}. *Bales et al.* [2001b] generated an accumulation map of the ice sheet, using historical data plus over 100 accurate point accumulation records developed since the 1991 map. Their ice sheet-wide accumulation estimate (30 g cm^2 a^{-1}) was basically the same as estimated by *Ohmura et al.* [1999]. Regionally, *Bales et al.* [2001b] estimated higher values in the central coastal areas and lower values in the south and west central areas. These maps were developed using estimates of solid precipitation from coastal weather stations to constrain interpolation of

[1]School of Engineering, University of California, Merced, California, USA.
[2]Sierra Nevada Research Institute, University of California, Merced, California, USA.
[3]Desert Research Institute, Reno, Nevada, USA.
[4]Department of Atmospheric and Climate Research, Norwegian Institute for Air Research, Kjeller, Norway.
[5]Earth Science Agency, Stateline, Nevada, USA.
[6]Department of Geography, University of Sheffield, Sheffield, UK.
[7]Danish Meteorological Institute, Copenhagen, Denmark.

0148-0227/09/2008JD011208$09.00

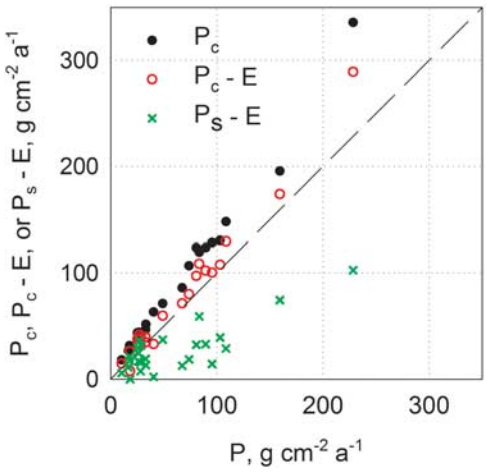

Figure 1. Precipitation for 20 coastal stations before versus after bias correction and calculation of solid precipitation.

accumulation values for the wet snow zone, with 39–86% of total annual precipitation at any one station falling in the solid form.

[4] The results from *Bales et al.* [2001a], based on kriging, also highlighted areas with higher uncertainty, particularly in the high-accumulation south central portion of the ice sheet. Subsequently, additional ice coring has been carried out to improve estimates in those areas [*Banta and McConnell*, 2007].

[5] The specific aim of the research reported in this paper was to update and improve estimates of accumulation across the ice sheet using recently developed ice core records, plus a more thorough analysis of coastal precipitation data. We also assess uncertainty in accumulation across the ice sheet.

2. Data and Methods

[6] Ice core and snow pit data were from 256 locations on the ice sheet previously compiled by *Bales et al.* [2001a] plus 39 ice core accumulation values developed since their compilation. Note that the 256 points from *Bales et al.* [2001a] were based on 158 historical points, developed by a dozen different groups using different methods in the period from the mid-1950s up through 1981, plus 99 high-quality point estimates developed by four groups since 1981. Their 158 historical values were a subset of 252 points compiled by *Ohmura and Reeh* [1991], with 98 of the points dropped because of large uncertainties associated with the methods used, set aside in favor of nearby points with longer records, or averaged with nearby points to yield a composite record. The primary coastal data used in the current analysis were daily values from 22 weather stations, reported by the Danish Meteorological Institute (DMI) [*Cappelen et al.*, 2001].

[7] Periodic gaps in the coastal data were filled using spatial correlation analysis. For each station with missing data we selected 2–4 neighboring stations, and using linear interpolation developed daily values for temperature, wind speed and precipitation. It should be recognized that while some neighboring points are over 200 km apart, they still provide the best estimate available for filling gaps. As two pairs of coastal points were within a few km of each other, and the records within each pair did not overlap, the 2 pairs were combined into 2 points. This averaging may in fact reduce local effects and provide a more regionally representative value for spatial interpolation. After data processing, each of the resulting 20 coastal points had at least 10 years of record. Biases of wind-induced undercatch, wetting loss and trace precipitation amounts were corrected on a daily basis using an algorithm developed for bias correction of daily precipitation for Greenland [*Yang et al.*, 1999]:

$$P_c = \frac{100}{\mathrm{CR}}\left(P_g + \Delta P_w + \Delta P_e\right) + \Delta P_t \qquad (1)$$

where P_c (mm) is corrected precipitation; P_g is gauge-measured precipitation; ΔP_w and ΔP_e are wetting loss and evaporation loss, respectively; ΔP_t is trace precipitation; and CR (%) is daily catch ratio, which is a function of the daily 6-h mean wind speed at the gauge height and precipitation type (Figure 1). Average wetting loss (ΔP_w) for each day precipitation occurred was assumed to be 0.10 mm for snow, 0.12 mm for mixed precipitation, 0.14 mm for rain [*Yang et al.*, 1999]. Actual wetting loss may be higher if multiple precipitation events occurred in a day. ΔP_e and ΔP_t were assumed to be zero and 0.1 mm, respectively, the same as reported by *Yang et al.* [1999].

[8] The fraction of solid precipitation was estimated following the empirical relation on Figure 2, which is adapted from *Ohmura et al.* [1999]. The fraction solid precipitation averaged 57% in our analysis (Table 1), versus 61% in *Ohmura et al.*'s [1999] analysis and 63% in *Ohmura and Reeh*'s [1991] analysis.

[9] The bias correction for the 20 stations averaged 47% (Table 1 and Figure 1). This compares well with the results of *Yang et al.* [1999], who reported corrections to the gauge-measured annual totals of 50–75% in the northern and 20–

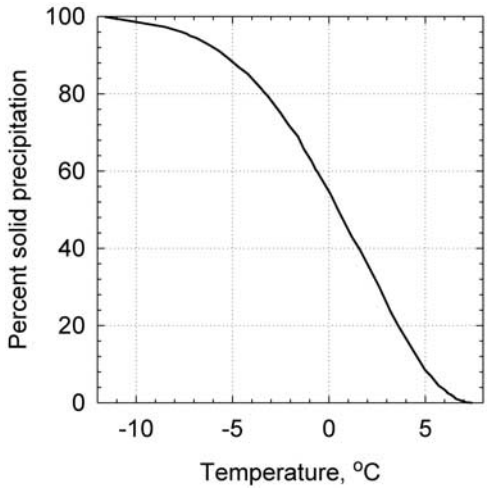

Figure 2. Relationship between temperature and solid precipitation. The original curve was created based on two data sets involving the individual synoptic observations from 17 Greenland stations and published by *Ohmura et al.* [1999]. In this study we digitized the original curve and fit it to a fifth-order polynomial to divide total precipitation into solid and liquid fractions. Precipitation was mixed between −11.6 and 7.4°C.

Table 1. Data for Coastal Stations in Greenland

Station	Period	Latitude	Longitude	P[a]	P_c[b]	P_c-E[c]	P_s[d]	P_s-E[e]
Qaqortoq	1961–2005	60.72	−46.05	95.5	128.3	100.3	42.4	14.4
Narsarsuaq Lufthavn	1961–2005	61.17	−45.42	67.4	86.0	71.4	27.3	12.7
Paamiut	1958–2001	62.00	−49.67	89.5	123.7	102.2	54.5	33.0
Nuuk	1958–2005	64.17	−51.75	80.8	123.8	97.2	59.0	32.4
Maniitsoql	1961–1986	65.40	−52.87	73.8	106.7	80.0	45.2	18.5
Kangerlussuaq	1976–2005	67.02	−50.70	18.4	26.9	7.5	12.0	−7.4
Aasiaat	1958–2005	68.70	−52.75	33.2	51.6	34.5	30.4	13.3
Ilulissat	1961–1990	69.22	−51.05	32.9	46.6	39.5	26.2	19.1
Upernavik	1958–1986	72.78	−56.17	28.4	43.5	31.6	27.8	15.8
Pituffik	1982–2005	76.53	−68.75	18.0	29.1	26.1	20.3	17.2
Station Nord	1961–1971, 1976–2005	81.60	−16.65	26.9	44.1	41.7	38.6	36.2
Danmarkshavn	1958–2005	76.77	−18.67	17.8	31.5	26.3	26.1	21.0
Daneborg	1958–1974	74.30	−20.22	25.3	43.6	37.6	35.2	29.3
Aputiteeq	1958–1973	67.78	−32.30	83.6	119.5	108.6	70.2	59.2
Tasiilaq	1958–2005	65.60	−37.63	103.2	130.4	107.7	62.0	39.3
Coastal1[f]	1961–1999, 2002–2004	66.94	−53.70	40.5	63.2	33.0	32.4	2.2
Coastal2[g]	1958–1979, 1982–2005	70.45	−21.96	49.0	71.2	59.7	48.7	37.2
Timmiarmiut	1958–1978	62.53	−42.13	159.4	195.5	173.8	96.4	74.6
Kangilinnguit	1961–1973	61.23	−48.10	108.7	147.9	129.6	47.1	28.9
Prins Christian Sund	1958–1979, 1993–2002, 2005	60.05	−43.17	228.4	335.6	289.1	149.2	102.7
Thule (Kanak)[h]	1956–1980[i]	77.48	−69.20	10.4	17.9	14.7	9.0	5.8
Mesters Vig[h]	1961–1974	72.25	−23.90	28.8	42.9	39.2	35.4	31.7
Umanak[h]	1951–1980	70.67	−52.00	16.7	26.5	16.6	21.0	11.2
Christianshab[h]	1962–1980	68.82	−51.08	26.1	39.2	33.4	22.6	16.8
Myggbukta[h]	1931–1939, 1946–1950	73.48	−21.57	26.3	39.5	32.7	31.2	24.4
Coastal3[h,j]	1931–1960	64.43	−50.25	28.2	42.0	31.6	17.9	7.5

[a]Precipitation before bias correction, g cm^{-2} a^{-1}.
[b]Precipitation after bias correction, g cm^{-2} a^{-1}.
[c]Where E is evaporation estimates.
[d]Solid precipitation after bias correction, g cm^{-2} a^{-1}.
[e]Accumulation, g cm^{-2} a^{-1}.
[f]Sisimiut (average of 4230 and 4234).
[g]Average of Illoqqortoormiut and Uunarteq.
[h]From *Bales et al.* [2001a].
[i]Data for 1961, 1962, 1963, 1965, and1977 are missing.
[j]Average of Neriunaq, Qornoq, and Kapsigdlit.

40% in the southern part of Greenland. *Ohmura et al.* [1999] reported an average bias correction of 18%, but used monthly rather than daily values of meteorological variables.

[10] *Bales et al.* [2001a] used 17 coastal points in their interpolation, based on the 40 records from individual weather stations reported by *Ohmura et al.* [1999]. The 17 coastal points were developed by combining colocated or nearby stations. Thus there was considerable overlap (11 points) between the coastal data used by *Bales et al.* [2001a] and the 20 DMI stations in the current analysis. Across those 11 points, precipitation before bias correction averaged 21.5% higher (ranging from 3.7% to 58.1% higher) in the current analysis as compared to *Bales et al.* [2001a], or about 5.3 g cm^{-2} a^{-1} higher. The other six historical coastal values used previously, which were not colocated with the 20 DMI points in the current analysis, were also used in the present Greenland-wide interpolation. These six points were corrected for bias based on the same relation as found for the DMI stations (Figure 1) and the reported relationship between corrected total precipitation and solid precipitation at each station [*Ohmura et al.*, 1999]. Thus 26 coastal points were used in the present analysis (Table 1).

[11] Evaporation was estimated for coastal sites from ERA-40 evaporation data, which were interpolated using inverse distance weighting based on 5-km resolution ERA-40 values from 1958 to 2005 using methods described previously by *Hanna et al.* [2006]. An extensive evaluation of ERA-40-based *P-E* using a subset of the shallow ice core and DMI coastal precipitation data used in this study suggested that ECMWF evaporation estimates, while first order, capture much of the spatial and temporal patterns of variability in Greenland [*Hanna et al.*, 2006].

[12] New ice core data (39 points) since *Bales et al.*'s [2001a] report were developed using methods described previously [*McConnell et al.*, 2000a, 2001] (Table 2). The accumulation measurements at most points span more than 10 years [*Hanna et al.*, 2006; *Banta and McConnell*, 2007].

[13] In some cases the new ice cores were at sites where historical records were available. In those cases we used the mean, more recent or longer period, i.e., the record that more accurately reflected long-term accumulation. Note that the period 1950–2000 is better represented by the data than are earlier periods. Among the 39 new ice core data, 7 points were used to replace points used by *Bales et al.* [2001a], and the other 32 points were added to the data series (Table 2). This resulted in a data series of accumulation with

Table 2. Recent PARCA Ice Core Data Developed Since Accumulation Estimates by *Bales et al.* [2001a]

Point	Latitude, Longitude	E^a	A^b	Period
NASAU[c]	73.8, −49.5	2352	34.3	1957–1994
GITS	77.1, −61.0	1868	34.4	1957–1995
HUMBOLDT[c]	78.5, −56.8	1998	14.7	1957–1994
CRAWPT	69.8, −47.1	1929	47.3	1982–1994
STUNU	69.8, −35.0	2929	47.6	1976–1996
7653[c]	76.0, −53.0	2186	34.8	1977–1996
DYE2	66.0, −46.0	2293	35.8	1957–1997
SDO2	63.1, −46.4	2715	53.3	1980–1998
CP1	69.9, −47.0	1974	35.8	1984–1998
CNP1	73.2, −32.1	3006	15.0	1957–1998
CNP2	71.9, −32.4	2795	22.3	1960–1998
CNP3	70.5, −33.5	2975	26.9	1964–1998
JAV2	72.6, −47.1	2644	38.8	1968–1998
JAV3	70.5, −46.1	2283	39.6	1981–1998
KUL1	67.5, −39.0	2475	51.9	1975–1998
UAK1[c]	65.5, −44.5	2561	47.3	1957–1998
UAK2	65.5, −43.5	2389	68.4	1984–1998
UAK4[c]	65.5, −46.1	2376	36.3	1977–1998
UAK5[c]	65.4, −46.5	2331	38.2	1978–1998
D1	64.5, −43.5	2648	74.8	1957–1998
D2	71.8, −46.2	2577	44.9	1957–1998
D3	69.8, −44.0	2467	41.6	1957–1998
SANDY	72.5, −38.3	3258	23.0	1957–2002
DAS1	66.0, −44.0	2549	60.0	1957–2002
DAS2	67.5, −36.1	3036	81.3	1957–2002
BASIN1	71.8, −42.4	2971	36.4	1976–2002
BASIN2	68.3, −44.8	2224	37.8	1980–2002
BASIN5	63.9, −46.4	2520	34.6	1964–2002
BASIN6	67.0, −41.7	2467	65.7	1983–2002
BASIN7	67.5, −40.4	2508	65.0	1983–2002
BASIN8	69.8, −36.4	3015	35.4	1957–2002
BASIN9	65.0, −44.9	2648	35.7	1957–2002
D5	68.5, −42.9	2519	38.1	1957–2002
D4	71.4, −44.0	2766	41.6	1957–2002
ACT1	66.5, −46.3	2145	36.1	1958–2003
ACT2	66.0, −45.2	2408	38.9	1957–2003
ACT3	66.0, −43.6	2508	68.0	1957–2003
ACT4	66.0, −42.8	2353	80.1	1979–2003
KATIE	72.6, −38.5	3252	22.4	1957–2003

[a]Elevation meters above sea level.
[b]Annual accumulation g cm^{-2} a^{-1}.
[c]The point was used to replace another point used by *Bales et al.* [2001a].

315 points in Greenland, 289 on the ice sheet and 26 coastal (Figure 3). None of the ice sheet accumulation estimates were based on a single year's measurement, in contrast to past data sets [*Bales et al.*, 2001a; *Ohmura and Reeh*, 1991] (Figure 4). While in a prior analysis [*Bales et al.*, 2001b] we adjusted the accumulation values from short records to the 1970–2000 time period based on decadal averages from longer records, we found the kriged result to be essentially the same with versus without the adjustment. Thus no adjustments were made in the current analysis.

[14] Using solid precipitation at coastal sites (P_S-E) plus the ice sheet data, a third-order trend was removed from the data and kriging was performed on the residuals. Subtraction of regional variability, e.g., using a third-order surface, is common to ensure intrinsic stationarity in the residuals, which is required for kriging. The trends were added back to the kriged residuals to estimate the final accumulation. Semivariograms were calculated at lag sizes of 10 km for 30 lags. A spherical model with a nugget of 20 (g cm^{-2} a^{-1})^2, a partial sill of 56 (g cm^{-2} a^{-1})^2, and a range of 200 km was estimated from the semivariograms. A search neighborhood with a search radius of 200 km involving 8 to 16 points for kriging was used.

[15] The variance for the whole interpolation domain was calculated as follows:

$$\mathrm{Var}(R(x_0)) = \hat{\sigma}_{AA}^2 + \sum_{i=1}^{n}\sum_{j=1}^{n} w_i w_j \hat{C}_{ij} - 2\sum_{i=1}^{n} w_i \hat{C}_{iA}$$

$$\sum W_i = 1 \qquad (2)$$

[16] Note that A is the whole study area. $\hat{\sigma}_{AA}$ represents the average covariance within A and is calculated by discretizing A into multiple points and averaging the covariances between all possible pairs of points; $\hat{C}_{ij}$ represents the covariance between the sample values at the ith location and the jth location; and $\hat{C}_{iA}$ represents the average covariance between sample at ith location and the entire A [*Isaaks and Srivastava*, 1989].

[17] Interpolation was also done using total rather than solid precipitation from coastal weather stations (P_c-E). In this case a third-order trend was also removed from the data. Semivariograms were calculated at lag sizes of 10 km for 30 lags. A spherical model with a nugget of 25 (g cm^{-2} a^{-1})^2, a partial sill of 80 (g cm^{-2} a^{-1})^2, and a range of 200 km was estimated from the semivariograms. The nuggets and partial sills of the P_c-E are greater than those of P_s-E, which are primarily due to the higher variance of P_c-E. A search neighborhood with a search radius of 200 km involving 8 to16 points for kriging was used.

3. Results

[18] The mean accumulation value of 289 ice core and snow pit points is 30.8 g cm^{-2} a^{-1}, with a standard error of 0.9 g cm^{-2} a^{-1}. The mean values for 26 coastal points are 26.8 g cm^{-2} a^{-1} (P_S-E) and 67.9 g cm^{-2} a^{-1} (P_c-E). Considering interannual variability, the mean coefficient of variation (CV) of the 39 new ice core records is 0.22, (range 0.11–0.36); the mean CV of P_S-E for the 20 coastal records is 0.31 (range 0.21–0.46); while for P_C-E the mean CV is 0.26 (range 0.17–0.39).

[19] On the basis of kriging, the average accumulation (±standard error) over the ice sheet portion of Greenland is 30.0 ± 1.2 g cm^{-2} a^{-1} (P_S-E), with a value of 29.0 ± 1.2 g cm^{-2} a^{-1} for all of Greenland. Using P_C-E, the respective values are 33.8 ± 2.9 and 35.4 ± 2.9 g cm^{-2} a^{-1}, fully 13 and 22% higher, respectively. Observed and modeled P_S-E values at all 315 points had the same means (30.5 g cm^{-2} a^{-1}), with an R^2 value of 0.9627. Note that kriging variance measures the standard errors of the predicted mean of a sample, and depends on the semivariogram and spatial configuration of the observations [*Foody and Atkinson*, 2002]. From the classical statistical context, the standard error is the standard deviation of the samples divided by square root of the number of independent measurements. For a 95% confidence level, the true value is expected to be within ±2 standard error; i.e., in this study, the average accumulation over the Greenland ice sheet is 30.0 ± 2.4 g cm^{-2} a^{-1} with a 95% confidence level.

[20] Accumulation generally increases from northern to southern Greenland, and is higher in southern coastal areas (Figures 5–6). Because the kriging, which was done

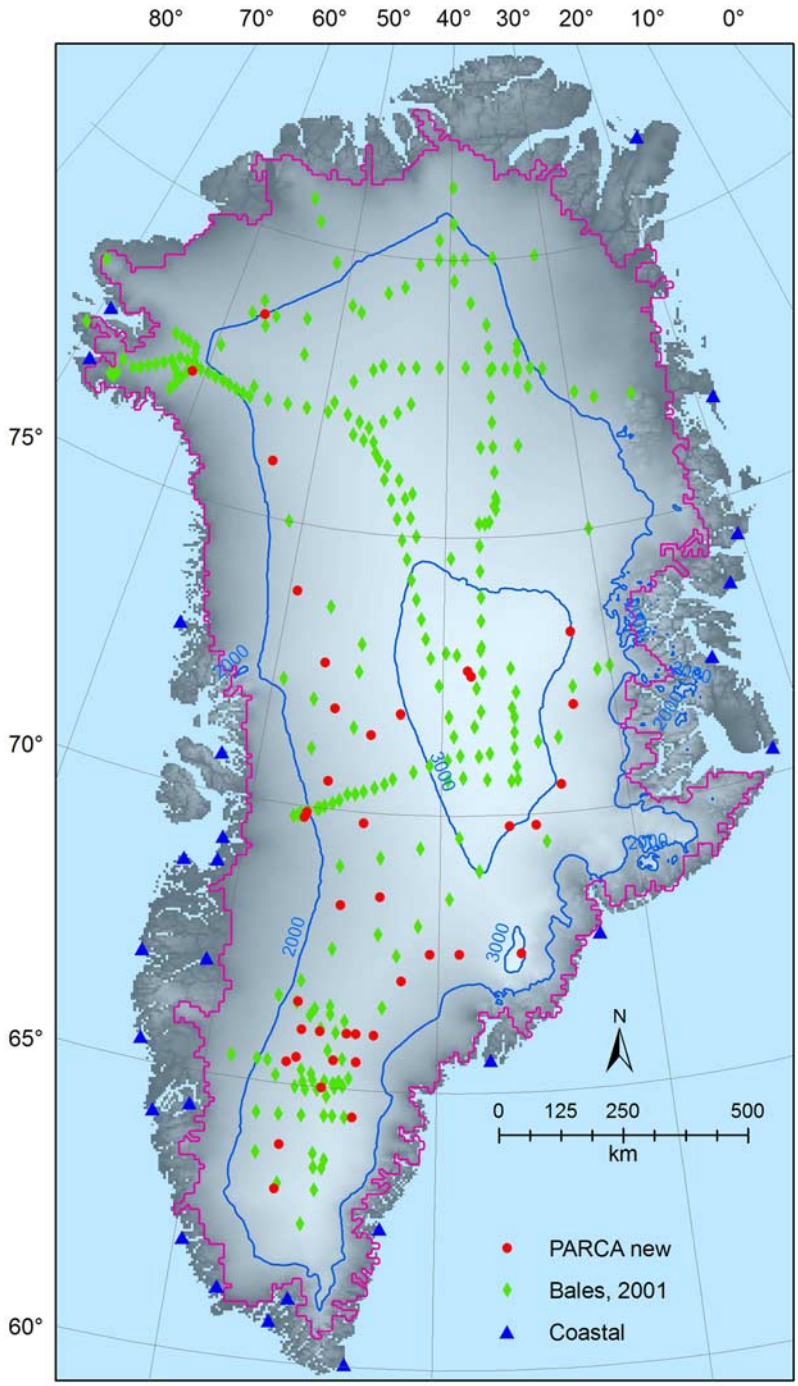

Figure 3. Data for kriging interpolation. Both data sets involve 39 new ice core data developed during 2000–2006 by the PARCA group, plus 250 ice core and snow pit data used by *Bales et al.* [2001a] (indicated as Bales, 2001 on image) and 26 coastal accumulation estimates (20 points reported by Danish Meteorological Institute (DMI) and 6 points used by *Ohmura et al.* [1999]).

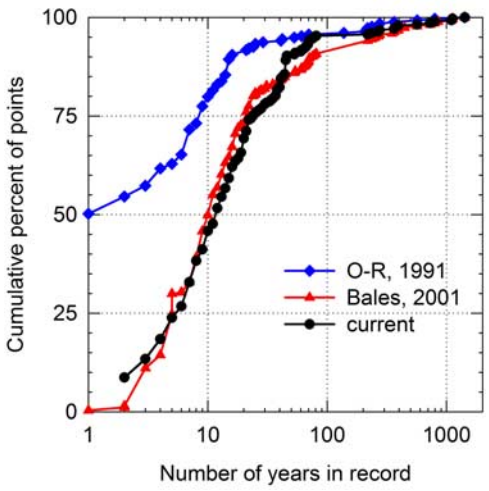

Figure 4. Distribution of record lengths for point accumulation estimates using ice cores and snow pits (Bales, 2001 data are from *Bales et al.* [2001a] and O-R, 1991 data are from *Ohmura and Reeh* [1991]).

on a 5-km grid, gave some discontinuities in the near-coastal areas where data are sparse, a 9 × 9 rectangular mean filter was applied to the images for mapping. This procedure effectively eliminated the discontinuities without changing the main features or regional kriged values [*Bales et al.*, 2001b].

4. Discussion

[21] It should be noted that standard errors for individual points are different from the standard error for the mean, and the former are normally greater than the latter. Figure 7 shows the distribution of standard error for individual points from kriging interpolation, which can highlight areas having the greatest uncertainty. In Figure 7, the range of the prediction standard error is 5.0–9.2 g cm^{-2} a^{-1}. Note that a spherical model with a nugget of 20 (g cm^{-2} a^{-1}) ^{2} was estimated from semivariograms, so the minimum possible prediction standard error would be ~4.5 g cm^{-2} a^{-1}, which mainly represents short-scale variability in accumulation [*McConnell et al.*, 2000b; *Banta and McConnell*, 2007], as measurement errors are small. The areas with lower prediction standard errors (5.0–7.0 g cm^{-2} a^{-1}) are centered on data points, whereas those with higher prediction standard errors (7.0–8.0 g cm^{-2} a^{-1}) are in areas with fewer data. Highest prediction standard errors (8.0–9.2 g cm^{-2} a^{-1}) are mainly in coastal regions with few data, while lower prediction standard errors are in the dry snow zone with elevation above 2000 m. The high standard errors near margins of the study area are also partially due to the fact that interpolation methods are not able to use all data points near the margins, which is referred to as "border effect" [*Tao*, 1995].

[22] In the current analysis of accumulation we have chosen to use only observations that we judged to be accurate and essentially free of bias. Regional climate models and reanalyses complement interpolation-based methods, and can improve our understanding of the physical mechanisms driving ice sheet surface balance [*Box et al.*, 2006; *Hanna et al.*, 2006]. Meanwhile, they offer the possibility of estimating mass balance over time and space, albeit introducing their own biases. We did evaluate use of regional reanalysis data to fill gaps in our observational data, but did not use them because of the further uncertainty that would be introduced into our estimates. While interpolation-based methods only provide a snapshot of accumulation, they are an important benchmark against which to evaluate the regional climate models.

[23] Uncertainties arise from (1) short-scale spatial variability in accumulation from sastrugi and other depositional processes [*Fisher et al.*, 1985], (2) changes in local topography, which can result in significant kilometer-scale variability [*Banta and McConnell*, 2007; *Spikes et al.*, 2004, 2007; *McConnell et al.*, 2000b], and (3) multiannual to multidecadal variability driven by large-scale circulation phenomena [*Appenzeller et al.*, 1998, *Hanna et al.*, 2006]. For example, *Banta and McConnell* [2007] analyzed annual accumulation measurements from eight of the longer, century-scale ice cores used in the current study and found short-scale spatial variability of ~3.7 g cm^{-2} a^{-1} (standard error) for parallel cores located within a few kilometers of each other near Summit, Greenland and medium-scale variability of ~4.9 g cm^{-2} a^{-1} for cores located a few hundred kilometers apart in west central Greenland. Coherent long-term variability for both regions was ~7% of the long-term mean accumulation, demonstrating that uncertainty is introduced when comparing accumulation measurements from different time periods. Analysis of closely spaced decadal-scale records from six core sites widely distributed around Greenland yielded similar short-scale spatial variability despite large differences in mean annual accumulation at the different core locations [*McConnell et al.*, 2000b]. Sets of cores from two sites in Greenland had spatial variability of 3.5–4.0 g cm^{-2} a^{-1} [*Anklin et al.*, 1998].

[24] Patterns in the 2001 Program for Arctic Regional Climate Assessment (PARCA) accumulation map (Figure 8) and the map developed in this study are very similar in most areas (Figure 9). There are five distinct regional differences between the two maps: southwest, northwest and eastern regions, where the accumulation values are lower than previously estimated; southeast and northeast regions, where the accumulation values are higher than previously estimated (Figure 9). Average accumulation in drainage basins 3–5 accounted for the main differences at the higher elevations on the ice sheet (Table 3 and Figure 9). Differences at lower elevations were greater. The new accumulation map retains the average features of the previous map (Table 4). The difference between the two maps is mainly in areas with elevation less than 2000 m, where the accumulation values are lower than previously estimated.

[25] In areas with elevation equal to or greater than 2000 m, the average accumulation is 29.9 g cm^{-2} a^{-1} while in those areas with elevation less than 1000 m, the average accumulation is 27.2 g cm^{-2} a^{-1}.

[26] The changes in spatial patterns of accumulation from earlier accumulation maps suggest that in some regions the Greenland ice sheet is closer to balance than previously estimated. For example, *Thomas et al.* [2001] and *Rignot et al.* [2004] both used a mass balance approach to determine long-term mass balance for specific catchments. They compared estimates of accumulation to discharge from the

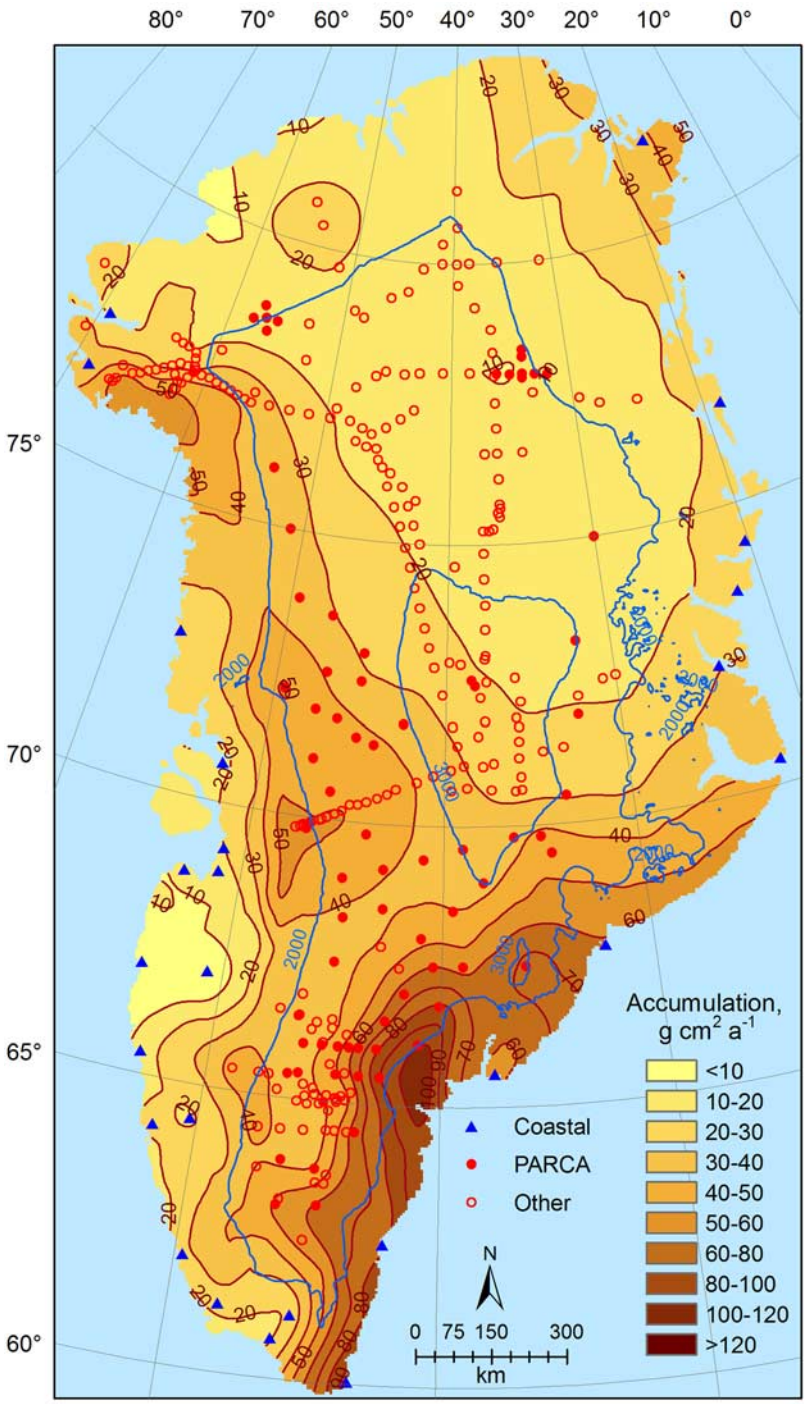

Figure 5. Accumulation prediction map based on kriging. Also shown for reference are the 2000-m and 3000-m elevation contours.

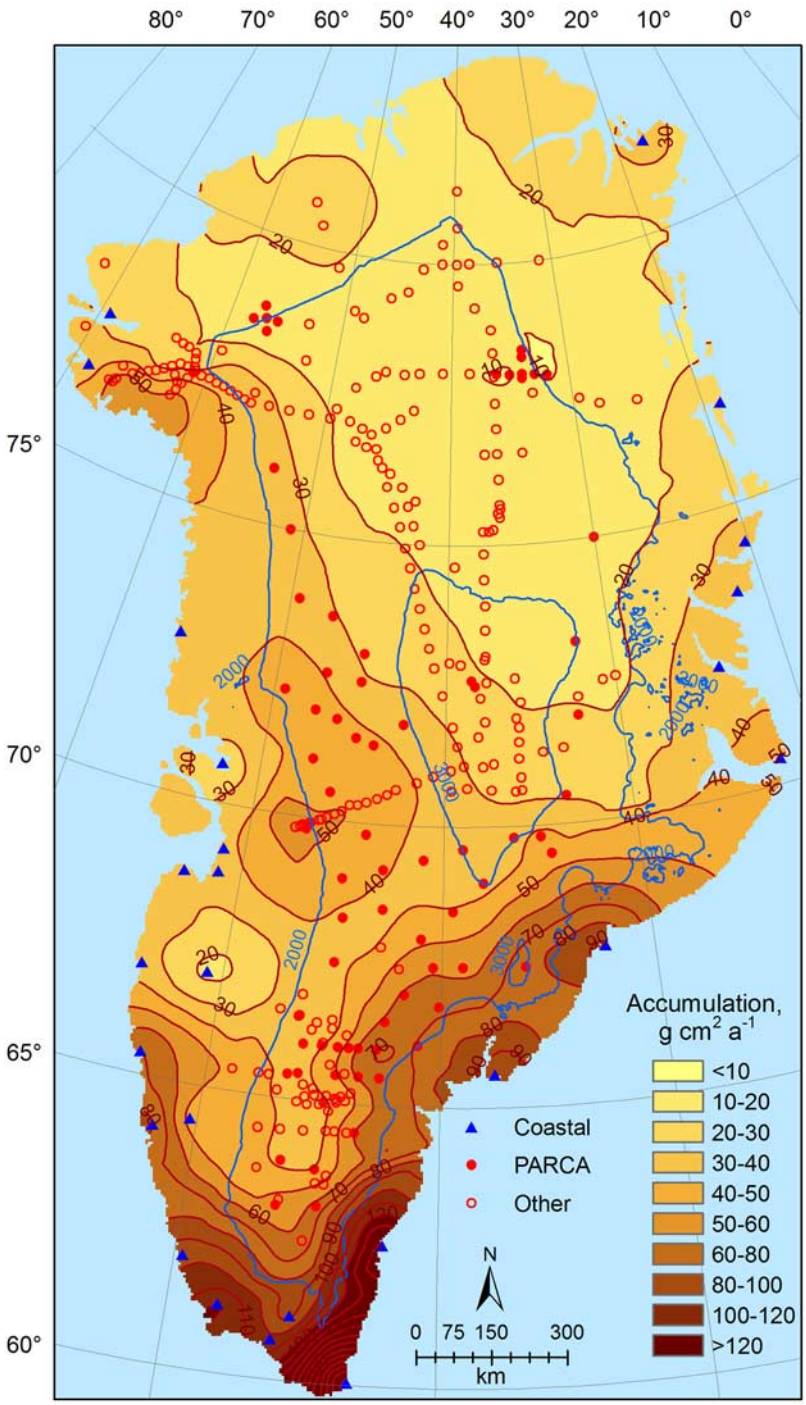

Figure 6. P_c-E prediction map based on kriging. Also shown for reference are the 2000-m and 3000-m elevation contours.

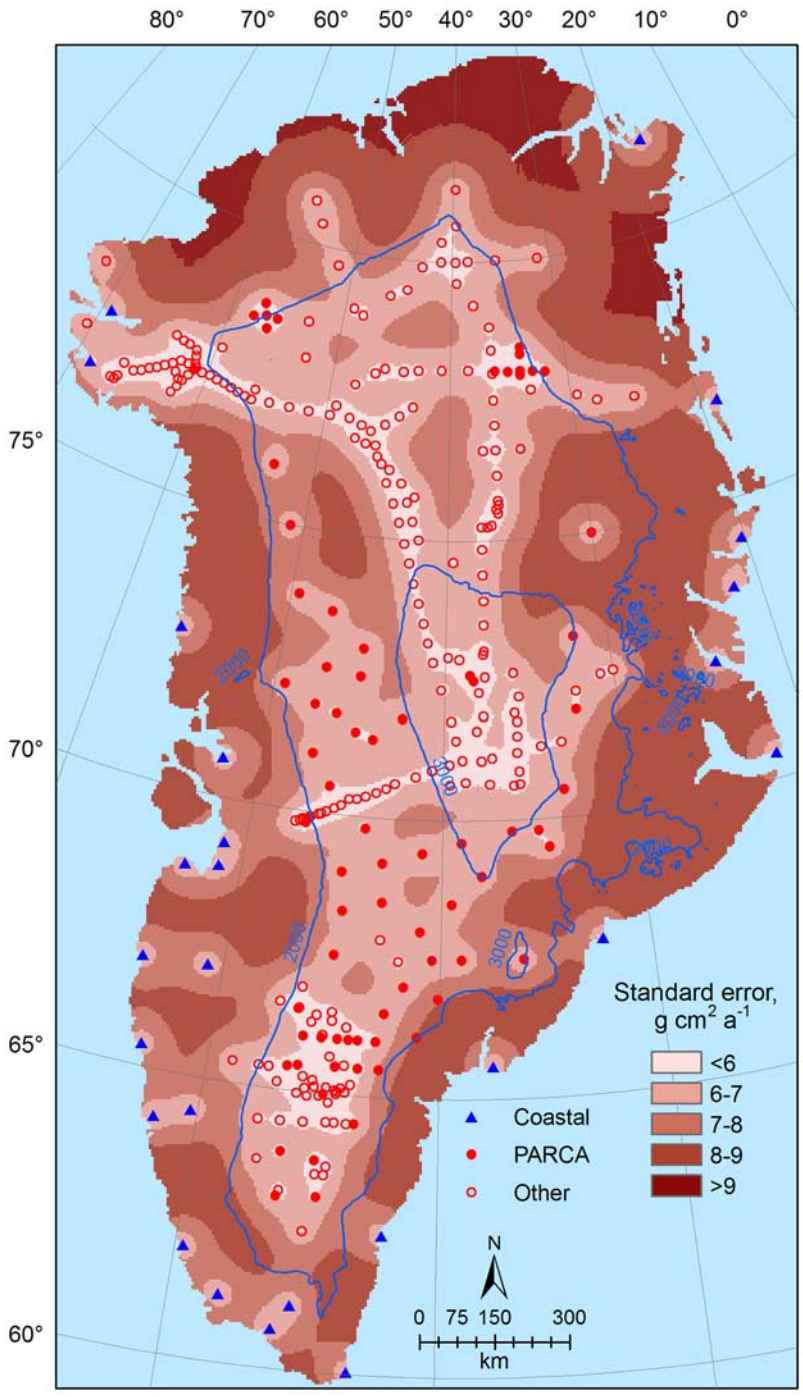

Figure 7. Accumulation prediction standard error map based on kriging. Also shown for reference are the points used to develop the kriged surface.

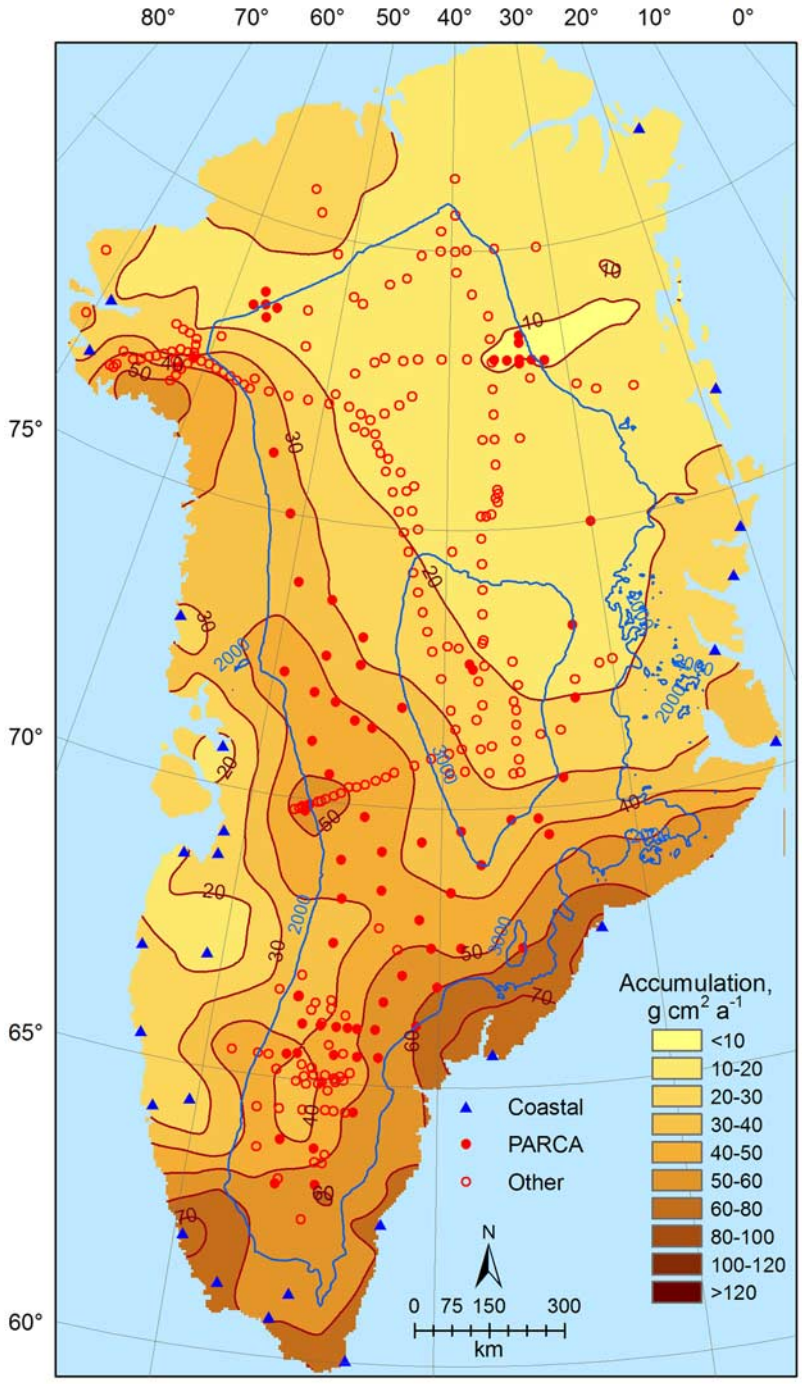

Figure 8. Accumulation map published by *Bales et al.* [2001a].

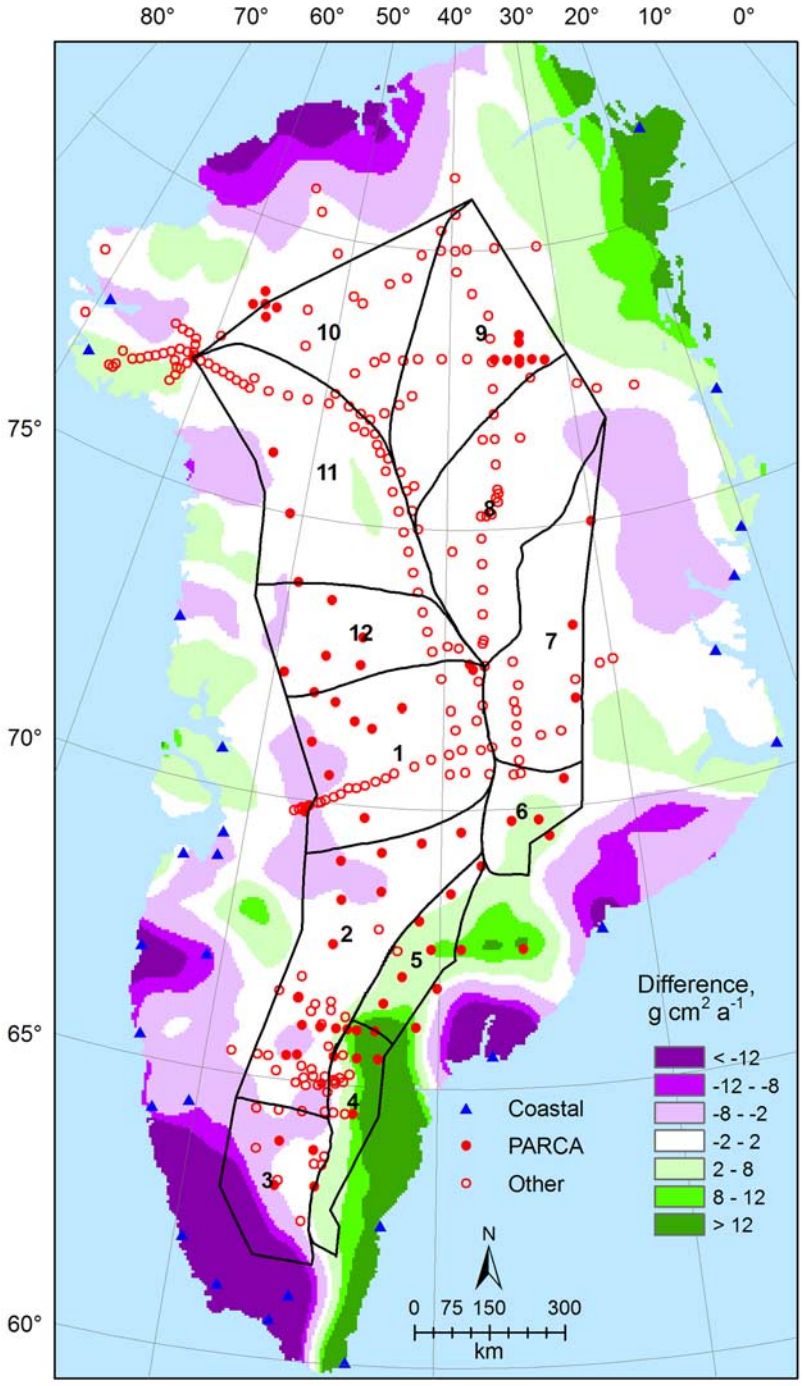

Figure 9. Difference between accumulation map in this research and that published by *Bales et al.* [2001a]. Also shown are ice cores and snow pits data used in current research and those used by *Bales et al.* [2001a] and the 2000-m and 3000-m elevation contours.

Table 3. Average Accumulation by Basin[a]

Basin	Map Values		
	P_c-E	P_s-E	P-E*[b]
1	38.1	37.7	38.4
2	39.6	39.0	40.0
3	54.2	42.4	49.1
4	63.2	60.7	52.0
5	55.7	55.2	49.7
6	35.4	35.6	34.3
7	18.4	18.0	18.2
8	13.8	13.3	13.9
9	12.5	12.3	12.3
10	15.5	15.2	15.4
11	26.8	27.2	27.4
12	32.5	32.0	32.5

[a]See Figure 9.
[b]*Bales et al.* [2001a].

catchments determined from surface velocity measurements near or below the equilibrium line. *Thomas et al.* [2001] found a strongly positive mass balance in the southwest (snowfall greatly exceeds discharge), and both *Thomas et al.* [2001] and *Rignot and Kanagaratnam* [2006] found a strongly negative mass balance in the southeast. The difference between the P-E* average for basin 3 (Table 3) of 49.1 g cm^{-2} a^{-1} [*Bales et al.*, 2001a] and P_s-E average of 42.4 g cm^{-2} a^{-1} equates to a reduction of 3.55 Gt a^{-1} in the estimate of net snow accumulation in the basin. Using the volume balance approach [*Thomas et al.*, 2001; *Rignot et al.*, 2004], this suggests an average long-term elevation rate change from mass imbalance in the basin of ~7.4 cm a^{-1}, similar to the 5.1 and 3.0 cm a^{-1} observed by laser and radar repeat altimetry, respectively. The earlier estimate of long-term thickening in the basin was 26.1 ± 5.2 cm a^{-1} [*Thomas et al.*, 2001].

[27] In the wet snow zone of the ice sheet, which lacks precipitation and accumulation measurements, the fraction of solid precipitation increases significantly in going from the coast inland over 50–100 km [*Box et al.*, 2006], but it is less clear how much total precipitation changes. *Taurisano et al.* [2004] reported that although coastal and glacier weather stations in the Nuuk area reported a 2–3°C difference in temperature, summer precipitation was similar at both sites, reflecting the combined effects of drier conditions inland counterbalanced with increased precipitation from orographic uplift (50 versus 750 m) over the 115 km distance. In Kangerlussuaq, there is a drop of nearly 57% in total precipitation in going inland from the coast, with little elevation change, though still an increase in the fraction of solid precipitation.

[28] Most of the precipitation on the ice sheet, even in the near-coastal margins, is solid (57 ± 17% for coastal stations in Table 1). However, it is not clear whether using accumulation based on total precipitation (Figure 6), solid precipitation (Figure 5) or something in between from coastal stations provides the best estimate of accumulation in the area of the ice sheet with no measurements. Differences between these two approaches average 12.6% of accumulation over the Greenland ice sheet. In the coastal, ice-free margin, liquid precipitation runs off rather than accumulates. That is true to some extent near the edges of the ice sheet as well, but some rainfall can be expected to refreeze and run off as part of the normal summer melting. *Ohmura and Reeh* [1991] suggest that using solid precipitation from coastal stations in the interpolation gives more realistic accumulation for elevations below 2000 m. They also note that after investigating both annual precipitation and accumulation for 12 glaciers, measured precipitation is on average 17% lower than accumulation, due in part to undercatch of solid precipitation in rain gages. For the 20 DMI stations, we found it to be 18% less, based on the corrections for gage loss and considering the solid fractions noted above (P_s/P).

[29] Ground-penetrating radar has the potential to extend accumulation measurements and thus to reduce uncertainty, particularly in lower elevation areas where some annual layering of physical properties is preserved but ice coring is not feasible due to wet snow. For example, one radar transect taken at 66°N (Figure 10) provides an excellent match to accumulation from seven ice cores taken along the traverse. Accumulation here exhibits the regular patterns observed in the longer traverses by *Benson* [1962]. ERA-40 results for the same radar transect show that modeling captures the general patterns of precipitation, but is not an accurate estimator of precipitation locally. Note that above 2000-m elevation, the interpolated accumulation based on P_s-E versus P_c-E values coincide in most regions, but diverge significantly within 100 km of the coast.

5. Conclusions

[30] In the inland areas the ice sheet, average accumulation (P_s–E) is almost the same as previously estimated. In the southwest, northwest and eastern parts of near-coastal areas the accumulation is generally lower than previously estimated; while in southeast and northeast parts of near-coastal areas the accumulation is generally higher than previously estimated. In basins 9–11, in the north, these differences are due entirely to addition of new coastal data and reanalysis of prior coastal data. The coastal data are largely responsible for differences across the central and southern portions of the ice sheet as well, with the new ice cores influencing values in these areas. However, the main effect of the new ice cores was to reduce uncertainty above 2000-m elevation. The uncertainty in our individual point measurements of accumulation is very low, and the 95% confidence interval from the kriging (±2.4 g cm^{-2} a^{-1}) likely represents an upper limit on uncertainty of ice sheet accumulation and can be reduced only through addressing areas where no measurements exist.

Table 4. Comparison of the Interpolation Results From Different Data Sources

Area[a]	Interpolation Results (g cm^{-2} a^{-1})		
	P_c-E	P_s-E	P-E*[b]
Greenland	35.4	29.0	29.8
Ice sheet	33.8	30.0	30.4
Elev ≥ 2000 m	31.4	29.9	29.8
1500 ≤ Elev < 2000 m	35.4	29.8	31.4
1000 ≤ Elev < 1500 m	38.5	29.3	30.9
Elev < 1000 m	41.4	27.2	29.2

[a]*E*, elevation.
[b]*Bales et al.* [2001a].

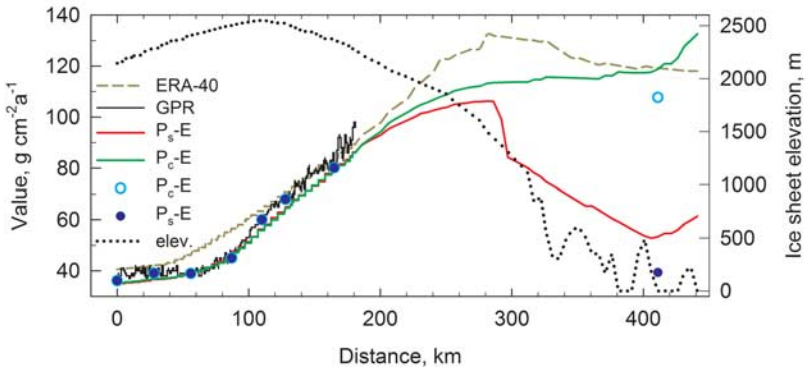

Figure 10. Accumulation based on ground-penetrating radar (GPR) [*Spikes et al.*, 2007] compared to estimates from 7 ice cores (P_s-E points). Also shown are values from accumulation maps (Figures 6–7) for the same transect, extending to the coast, and ERA-40 values for the same transect. Both P_s-E and P_c-E are shown for the coastal station.

[31] The much lower accumulation in the southwest and much higher in the southeast indicated by the current map means that long-term mass balance in both catchments is closer to steady state than previously estimated, and is more in line with repeat altimetry. However, uncertainty in these areas remains high owing to strong gradients in precipitation from the coast inland. It is likely that accumulation is underestimated in this zone. A significant and sustained measurement program will be needed to resolve this uncertainty.

[32] **Acknowledgments.** We acknowledge NASA grant NNG04GB26G to University of California, Merced; NASA grants NAG5–12752 and NAG04GI66G; and NSF grant OPP-0221515 to the Desert Research Institute.

References

Anklin, M., R. C. Bales, E. Mosley-Thompson, and K. Steffen (1998), Annual accumulation at two sites in northwest Greenland during recent centuries, *J. Geophys. Res.*, *103*(D22), 28,775–28,783, doi:10.1029/98JD02718.

Appenzeller, C., T. F. Stocker, and M. Anklin (1998), North Atlantic Oscillation dynamics recorded in Greenland ice cores, *Science*, *282*, 446–449, doi:10.1126/science.282.5388.446.

Bales, R. C., J. R. McConnell, E. Mosley-Thompson, and B. Csatho (2001a), Accumulation over the Greenland ice sheet from historical and recent records, *J. Geophys. Res.*, *106*(D24), 33,813–33,825, doi:10.1029/2001JD900153.

Bales, R. C., J. R. McConnell, E. Mosley-Thompson, and G. Lamorey (2001b), Accumulation map for the Greenland ice sheet: 1971–1990, *Geophys. Res. Lett.*, *28*(15), 2967–2970, doi:10.1029/2000GL012052.

Banta, J. R., and J. R. McConnell (2007), Annual accumulation over recent centuries at four sites in central Greenland, *J. Geophys. Res.*, *112*, D10114, doi:10.1029/2006JD007887.

Benson, C. S. (1962), Stratigraphic studies in the snow and firn of the Greenland ice sheet, *SIPRE Res. Rep. 70*, U.S. Army Snow, Ice and Permafrost Res. Estab., Corps of Eng., Wilmette, Ill.

Box, J. E., D. H. Bromwich, B. A. Veenhuis, L.-S. Bai, J. C. Stroeve, J. C. Rogers, K. Steffen, T. Haran, and S.-H. Wang (2006), Greenland ice sheet surface mass balance variability (1988–2004) from calibrated Polar MM5 output, *J. Clim.*, *19*, 2783–2800, doi:10.1175/JCLI3738.1.

Cappelen, J., B. V. Jorgensen, E. V. Laursen, L. S. Stannius, and R. S. Thomsen (2001), The observed climate of Greenland, 1958–99–with climatological standard normals, 1961–90, *Tech. Rep. 00-18*, Dan. Meteorol. Inst., Copenhagen, Denmark.

Davis, C. H., Y. Li, J. R. McConnell, M. M. Frey, and E. Hanna (2005), Snowfall-driven growth in East Antarctic Ice Sheet mitigates recent sea-level rise, *Science*, *308*, 1898–1901, doi:10.1126/science.1110662.

Fisher, D. A., N. Reeh, and H. B. Clausen (1985), Stratigraphic noise in time series derived from ice cores, *Ann. Glaciol.*, *7*, 76–83.

Foody, G. M., and P. M. Atkinson (Eds.) (2002), *Uncertainty in Remote Sensing and GIS*, 307 pp., John Wiley, Chichester, U. K.

Hanna, E., J. McConnell, S. Das, J. Cappelen, and A. Stephens (2006), Observed and modelled Greenland ice sheet snow accumulation, 1958–2003, and links with regional climate forcing, *J. Clim.*, *19*, 344–358, doi:10.1175/JCLI3615.1.

Hanna, E., P. Huybrechts, K. Steffen, J. Cappelen, R. Huff, C. Shuman, T. Irvine-Fynn, S. Wise, and M. Griffiths (2008), Increased runoff from melt from the Greenland ice sheet: A response to global warming, *J. Clim.*, *21*, 331–341, doi:10.1175/2007JCLI1964.1.

Hanna, E., J. Cappelen, X. Fettweis, P. Huybrechts, A. Luckman, and M. H. Ribergaard (2009), Hydrologic response of the Greenland ice sheet: The role of oceanographic warming, *Hydrol. Processes*, *23*, 7–30, doi:10.1002/hyp.7090.

Isaaks, E. H., and R. M. Srivastava (1989), *An Introduction to Applied Geostatistics*, 561 pp., Oxford Univ. Press, Oxford, U. K.

McConnell, J. R., R. J. Arthern, E. Mosley-Thompson, C. H. Davis, R. C. Bales, R. Thomas, J. F. Burkhart, and J. D. Kyne (2000a), Changes in Greenland ice-sheet elevation attributed primarily to snow-accumulation variability, *Nature*, *406*, 877–879, doi:10.1038/35022555.

McConnell, J. R., E. Mosley-Thompson, D. H. Bromwich, R. C. Bales, and J. D. Kyne (2000), Interannual variations of snow accumulation on the Greenland Ice Sheet (1985–1996): New observations versus model predictions, *J. Geophys. Res.*, *105*(D3), 4039–4046, doi:10.1029/1999JD901049.

McConnell, J. R., G. Lamorey, E. Hanna, E. Mosley-Thompson, R. C. Bales, D. Belle-Oudry, and J. D. Kyne (2001), Annual net snow accumulation over southern Greenland from 1975 to 1998, *J. Geophys. Res.*, *106*(D24), 33,827–33,837, doi:10.1029/2001JD900129.

Ohmura, A., and N. Reeh (1991), New precipitation and accumulation maps for Greenland, *J. Glaciol.*, *37*(125), 140–148.

Ohmura, A., P. Calanca, M. Wild, and M. Anklin (1999), Precipitation, accumulation and mass balance of the Greenland Ice sheet, *Z. Gletscherkd. Glazialgeol.*, *35*(1), 1–20.

Rignot, E., and S. Kanagaratnam (2006), Changes in the velocity structure of the Greenland ice sheet, *Science*, *311*, 986–990, doi:10.1126/science.1121381.

Rignot, E., S. P. Gogineni, P. Kanagaratnam, W. B. Krabill, and J. R. McConnell (2004), Rapid ice discharge from southeast Greenland glaciers, *Geophys. Res. Lett.*, *31*, L10401, doi:10.1029/2004GL019474.

Spikes, V. B., G. S. Hamilton, S. A. Arcone, S. Kaspar, and P. A. Mayewski (2004), Variability in accumulation rates from GPR profiling on the West Antarctic Plateau, *Ann. Glaciol.*, *39*, 238–244, doi:10.3189/172756404781814393.

Spikes, V. B., J. R. McConnell, and J. R. Banta (2007), Annual layer mapping and net snowfall measurements across the southern Greenland ice sheet using shallow radar and ice cores, *Eos Trans. AGU*, *88*(52), Fall Meet. Suppl., Abstract C11A-0087.

Tao, S. (1995), Kriging and mapping of copper, lead, and mercury contents in surface soil in Shenzhen area, *Water Air Soil Pollut.*, *83*, 161–172, doi:10.1007/BF00482601.

Taurisano, A., C. E. Boggild, and H. G. Karlsen (2004), A century of climate variability and climate gradients from coast to ice sheet in West Greenland, *Geogr. Ann., Ser. A*, *86*, 217–224, doi:10.1111/j.0435-3676.2004.00226.x.

Thomas, R., B. Csatho, C. Davis, C. Kim, W. Krabill, S. Manizade, J. McConnell, and J. Sonntag (2001), Mass balance of higher-elevation parts of the Greenland ice sheet, *J. Geophys. Res.*, *106*(D24), 33,707–33,716, doi:10.1029/2001JD900033.

Yang, D., S. Ishida, B. E. Goodison, and T. Gunther (1999), Bias correction of daily precipitation measurements for Greenland, *J. Geophys. Res.*, *104*(D6), 6171–6181, doi:10.1029/1998JD200110.

Zwally, H. J., W. Abdalati, T. Herring, K. Larson, J. Saba, and K. Steffen (2002), Surface melt-induced acceleration of Greenland ice-sheet flow, *Science*, *297*, 218–222, doi:10.1126/science.1072708.

R. C. Bales, Sierra Nevada Research Institute, University of California, P.O. Box 2039, Merced, CA 95344, USA. (rbales@ucmerced.edu)

J. F. Burkhart, Department of Atmospheric and Climate Research, Norwegian Institute for Air Research, NO-2027 Kjeller, Norway.

J. Cappelen, Danish Meteorological Institute, Lyngbyvej 100, DK-2100 Copenhagen, Denmark.

G. Du, Q. Guo, and D. Shen, School of Engineering, University of California, P.O. Box 2039, Merced, CA 95344, USA.

E. Hanna, Department of Geography, University of Sheffield, Winter Street, Sheffield S10 2TN, UK.

J. R. McConnell, Desert Research Institute, 2215 Raggio Parkway, Reno, NV 89512, USA.

V. B. Spikes, Earth Science Agency, P.O. Box 2858, 275 Kingsbury Grade, Stateline, NV 89449, USA.